Cancer Research

Circulating Glioma Cells Exhibit Stem Cell-like Properties

Tianrun Liu[1,2], Haineng Xu[1], Menggui Huang[1], Wenjuan Ma[1,3], Deeksha Saxena[1], Robert A. Lustig[1], Michelle Alonso-Basanta[1], Zhenfeng Zhang[4], Donald M. O'Rourke[5], Lin Zhang[6], Yanqing Gong[7], Gary D. Kao[1], Jay F. Dorsey[1], and Yi Fan[1,5]

Abstract

Circulating tumor cells (CTC) are known to be present in the blood of patients with glioblastoma (GBM). Here we report that GBM-derived CTC possess a cancer stem cell (CSC)-like phenotype and contribute to local tumorigenesis and recurrence by the process of self-seeding. Genetic probes showed that mouse GBM-derived CTC exhibited Sox2/ETn transcriptional activation and expressed glioma CSC markers, consistent with robust expression of stemness-associated genes including SOX2, OCT4, and NANOG in human GBM patient-derived samples containing CTC. A transgenic mouse model demonstrated that CTC returned to the primary tumor and generated new tumors with enhanced tumorigenic capacity. These CTCs were resistant to radiotherapy and chemotherapy and to circulation stress-induced cell apoptosis. Single-cell RNA-seq analysis revealed that Wnt activation induced stemness and chemoresistance in CTC. Collectively, these findings identify GBM-derived CTC as CSC-like cells and suggest that targeting Wnt may offer therapeutic opportunities for eliminating these treatment-refractory cells in GBM.

Significance: These findings identify CTCs as an alternative source for *in situ* tumor invasion and recurrence through local micrometastasis, warranting eradication of systemic "out-of-tumor" CTCs as a promising new therapeutic opportunity for GBM. *Cancer Res; 78(23); 6632–42. ©2018 AACR.*

Introduction

Circulating tumor cells (CTC), tumor cells that have been shed into the vasculature or lymphatics from a primary tumor and enter the systemic circulation, play a fundamental role in cancer invasion, metastasis, and recurrence (1–4). CTCs can seed, proliferate, and colonize to form secondary tumors in proximal and distal sites. Likewise, as a potential clinical biomarker, the detection of CTCs has correlated with poor prognosis, lack of treatment response, or rapid tumor recurrence in patients with a variety of cancers including glioblastoma (GBM; refs. 5–8). However, the biological mechanism(s) underlying their contribution to tumorigenesis remains largely unknown. Understanding this contribution may serve to uncover new therapeutic targets to prevent cancer progression and recurrence.

GBM, grade IV glioma, is the most common and most aggressive primary brain tumor. GBM is among the most lethal of human malignancies, with a current median overall survival of approximately 16 months (9, 10). Despite aggressive standard-of-care treatments including surgical resection, radiation, and chemotherapy, recurrence of GBM is essentially universal, and recurrent tumors are highly resistant to conventional cytotoxic treatments. It is highly suggested that treatment-resistant glioma cells, particularly cancer stem cells (CSC), that is, tumor-initiating cells or tumor-propagating cells, contribute to the GBM recurrence. Here we show glioma CTCs acquire a CSC-like phenotype: activated in stemness, resistant to genotoxic treatments, and more importantly, able to home to a primary tumor site to repopulate locally and contribute to new tumor formation. Taken together, this suggests a previously unidentified role of CTCs for tumor micrometastasis and local relapse in GBM.

Materials and Methods

Patient-derived samples containing CTCs

Patients with GBM or non–small cell lung carcinoma (NSCLC) were treated at the Department of Radiation Oncology and Department of Neurosurgery of the Hospital of the University of Pennsylvania. Written informed consent was obtained from each patient. The studies were conducted in accordance with recognized ethical guidelines (Declaration of Helsinki, CIOMS,

[1]Department of Radiation Oncology, University of Pennsylvania Perelman School of Medicine, Philadelphia, Pennsylvania. [2]Division of Head and Neck Surgery, Department of Otorhinolaryngology, The Sixth Affiliated Hospital of Sun Yat-sen University, Guangzhou, China. [3]Department of Medical Oncology, State Key Laboratory of Oncology in South China & Collaborative Innovation Center for Cancer Medicine, Sun Yat-sen University Cancer Center, Guangzhou, China. [4]Department of Radiology, The Second Affiliated Hospital of Guangzhou Medical University, Guangzhou, China. [5]Department of Neurosurgery, University of Pennsylvania Perelman School of Medicine, Philadelphia, Pennsylvania. [6]Department of Obstetrics and Gynecology, University of Pennsylvania Perelman School of Medicine, Philadelphia, Pennsylvania. [7]Division of Human Genetics and Translational Medicine, Department of Medicine, University of Pennsylvania Perelman School of Medicine, Philadelphia, Pennsylvania.

Note: Supplementary data for this article are available at Cancer Research Online (http://cancerres.aacrjournals.org/).

T. Liu and H. Xu are co-first authors.

Corresponding Authors: Yi Fan, University of Pennsylvania, 3400 Civic Center Blvd, SCTR Rm 8-132, Philadelphia, PA 19104. Phone: 215-898-9291; Fax: 215-898-0090; E-mail: fanyi@uphs.upenn.edu; and Jay F. Dorsey, Jay.Dorsey2@uphs.upenn.edu

doi: 10.1158/0008-5472.CAN-18-0650

Belmont Report, and U.S. Common Rule) and approved by the University of Pennsylvania Institutional Review Board. The blood samples were collected under an Institutional Review Board–approved protocol. CTCs were genetically labeled and isolated as previously described. Ten milliliters of blood was diluted with equal volume of PBS, and transferred and separated via Oncoquick tube. After centrifugation at 400 x *g* for 35 minutes, the layer solution containing CTCs between the Ficoll and the blood was collected. The cells were collected by centrifugation at 400 x *g* for 35 minutes, and resuspended in 900 μL of DMEM media (Invitrogen) supplemented with 5% FBS (Invitrogen), 1.0% penicillin-streptomycin (Invitrogen). The hTERT promoter activity-based conditional replicated adenovirus (Oncolys BioPharma) was utilized to label the CTCs as previously described (7). Cells were incubated with 2×10^8 viral particles for 24, 48, and 72 hours in chamber slides (BD Biosciences). The cells were harvested by using a capillary-based vacuum-assisted cell acquisition system (Kuiqpick, NeuroInDx). Calibration was initially performed under bright and fluorescence field condition, and then pick up the selected cells (via micro-capillary aspiration) under fluorescence microscopy.

RCAS GBM mouse model

GBM was induced in mice as previously described (11, 12). In brief, chicken DF-1 fibroblasts (ATCC) were transfected with RCAS-PDGF-B and RCAS-Cre plasmids to produce retrovirus, and then orthotopically injected into the brain of *Ntv-a*;*Ink4a-Arf*$^{-/-}$;*Pten*$^{fl/fl}$;*LSL-luc* mice to induce GBM through RCAS/n-tva-mediated gene transfer. Tumorigenesis in brain was detected by bioluminescence imaging. Tumor growth was monitored by whole-body bioluminescence using an IVIS 200 Spectrum Imaging System (Perkin Elmer) after retro-orbital injection of D-luciferin (150 mg/kg; GoldBio). Tumors were isolated and subjected to mechanical dissociation with a gentleMACS Dissociator (Miltenyi), and enzymatic digestion with collagenase II and dispase II to obtain single cell suspensions. To analyze stemness transcriptional activation in CTCs, the tumor cells were transduced with lentivirus that encodes Sox2/Etn-GFP, followed by orthotopic injection (10^5 tumor cells/mouse) into wild-type C57BL/6 mice (8-weeks old, half male and half female; The Jackson Laboratory).

Isolation and culture of mouse CTCs

The isolation and labeling CTCs were performed in a protocol similar to isolation of human CTC as described above (7). In brief, 1 mL of blood or tumor cell suspension was collected from each GBM-bearing mice, diluted with equal volume of PBS, and layered over Ficoll solution. After centrifugation, the layer solution between the Ficoll and the blood was collected. The cells were collected by centrifugation, and resuspended in serum-free Neurobasal-A medium (Gibco), and cultured for 3 days in a humidified hypoxic atmosphere with 1% O_2 and 5% CO_2. Cells were then incubated with 2×10^8 viral particles for 2 days in chamber slides (BD Biosciences), followed by single-cell pickup of mCherry-expressing cells using the Kuiqpick cell acquisition system. The collected mouse CTCs and matched primary tumor cells were maintained in serum-free Neurobasal-A medium (Gibco), supplemented with B-27 Supplement Minus Vitamin A (Gibco), GlutaMax (Gibco), sodium pyruvate (Gibco), fibroblastic growth factor (FGF, 5 ng/mL; R&D Systems), and EGF (20 ng/mL; R&D Systems).

Human GBM CSC culture

Human patient-derived IN528 glioma CSCs were kindly provided by Dr. Jeremy Rich (University of California at San Diego, La Jolla, CA; refs. 13–15). The matched non-CSCs were generated by brief treatment with serum (10% FBS)-containing medium for 24 hours, and cultured back in stem cell medium as described previously (16). CSCs were cultured in serum-free Neurobasal-A medium (Gibco), supplemented with B-27 Supplement Minus Vitamin A (Gibco), GlutaMax (Gibco), sodium pyruvate (Gibco), fibroblastic growth factor (FGF, 5 ng/mL; R&D Systems), and EGF (20 ng/mL; R&D Systems).

Syngeneic glioma model

The CTCs or primary tumor cells (10^5 cells for each mouse) were subcutaneously injected into the right and left flank sites of C57BL/6 mice (8-weeks old; The Jackson Laboratory half male and half female). In addition, these cells (10^4 cells for each mouse) were intracranially injected into mouse brains, as previously descried (12). Tumor growth was monitored by whole-body bioluminescence using an IVIS 200 Spectrum Imaging System (Perkin Elmer) after retro-orbital injection of D-luciferin (150 mg/kg; GoldBio). The size of tumors was measured every week by using a caliper and the volume calculated.

CTC homing analysis

GBM was induced in *Ntv-a*;*Ink4a-Arf*$^{-/-}$;*Pten*$^{fl/fl}$;*LSL-luc* mice through RCAS/n-tva-mediated gene transfer. Cultured CTC cells were lentivirally transduced to co-express GFP and rLuc, and prepared as single-cell suspensions in PBS (2×10^6 cells/mL). Mice were anesthetized by intraperitoneal injection of ketamine/xylazine cocktail (ketamine 100 mg/kg, xylazine 10 mg/kg), and injected with 100 μL CTC cell suspension through carotid artery. Ten days after injection, mice were imaged by whole-body bioluminescence using an IVIS 200 Spectrum Imaging System (Perkin Elmer) after retro-orbital injection of coelenterazine (4 mg/kg; Promega), followed by secondary imaging after retro-orbital injection of D-luciferin (150 mg/kg; GoldBio). The tumors were excised and subjected to IHC analysis.

Quantitative real-time PCR analysis of human single cells

mRNA was isolated from harvested single cells including human CTCs, human glioma U251 cells by using an RNeasy Mini Kit (Qiagen). Quantitative real-time PCR was performed in a 20-μL reaction volume using Fast SYBR Green Master Mix (Applied Biosystems) and primers: Oct4 (FP: 5′- GTGGAGGAGCTGACAACAA -3′, RP: 5′- ATTCTCCAGGTTGCCTCTCA -3′), Sox2 (FP: 5′- CCCCCGGCGGCAATAGCA -3′, RP: 5′- TCGGCGCCGGGGAGATACAT -3′), Nanog (FP: 5′- CAAAGGCAAACAACCCACTT-3′, RP: 5′- TCTGCTGGAGGCTGAGGTAT-3′), BTRC (FP: 5′-CTGCAGGGACACTCTGTCTAC -3′, RP: 5′-GAAGTCCCAGATGAGGATTGTG-3′), CCND1 (FP: 5′-TCAAGTGTGACCCGGACTGC-3′, RP: 5′-CAGGTCCACCTCCTCCTCCT-3′), CCND2 (FP: 5′-CCACCGTCGATGATCGCAAC-3′, RP: 5′-GAGGAGCACCGCCTCAATCT-3′), FGF9 (FP: 5′-AGACCACAGCCGATTTGGCA -3′, RP: 5′-CCTTCCAGTGTCCACGTGCT -3′), GAPDH (FP: 5′-GTCTCCTCTGACTTCAACAGCG-3′, RP: 5′-ACCACCCTGTTGCTGTAGCCAA -3′).

RNA sequencing

GBM was induced in *Ntv-a*;*Ink4a-Arf*$^{-/-}$;*Pten*$^{fl/fl}$;*LSL-Luc* mice through RCAS/n-tva-mediated gene transfer. Tumors and blood

were collected, and single-cell CTCs and matched tumor cells (5–8 cells/mouse) were harvested and pooled. Cells were lyzed in Hank's Balanced Salt Solution buffer (Thermo Fisher) with 0.025% Tween (Thermo Fisher). mRNA was extracted and subjected to aRNA linear amplification by three rounds of reverse transcription, second strand synthesis and *in vitro* transcription, according to a previously published protocol (17), using SuperScript III First-Strand Synthesis SuperMix (Thermo Fisher), DNA Polymerase I (Thermo Fisher), T4 DNA polymerase (Thermo Fisher), 5x Second Strand buffer (Thermo Fisher), and a MegaScript Kit (Thermo Fisher). DNA library was constructed with a TruSeq mRNA Stranded Kit (Illumina). The RNA from each step and library DNA quality were analyzed with RNA Nano assay chips, RNA Pico assay chips, and DNA Nano assay chips using a 2100 bioanalyer (Agilent). Library was subjected to next-generation sequencing analysis in a high-throughput sequencing center with a HiSeq4000 at the Children's Hospital of Philadelphia/Beijing Genomics Institute core facility (CHOP/BGI). The sequences were aligned to the GRCm38 reference genome using RNA-Star (v2.4.2a; https://github.com/alexdobin/STAR). The gene expression was normalized and calculated as FPKM (Fragments Per Kilobase Million) values by Cufflinks (v2.2.1) (http://cole-trapnell-lab.github.io/cufflinks/releases/v2.2.1/) with Gencode M5 gene annotations (https://www.gencodegenes.org/mouse/release_M5.html). RNA-seq data have been deposited in NCBI's Gene Expression Omnibus under the accession GSE120776.

Flow cytometry

GBM was induced in *Ntv-a;Ink4a-Arf*$^{-/-}$;*Pten*$^{fl/fl}$;*LSL-luc* mice through RCAS/n-tva-mediated gene transfer. Tumors were excised. Single-cell tumor suspension was transduced with lentivirus that encodes Sox2/Etn-GFP or promoter-free sequence. The cells were subjected to flow cytometry analysis with an Accuri C6 flow cytometer (BD Biosciences) by using FlowJo software.

In vitro circulation system

Mouse CTCs and tumor cells were cultured in serum-free Neurobasal-A. A total of 2×10^6 cells in 30 mL medium were transferred into an *in vitro* circulation system with a fluid circulation rate of 80 mL/min. The circulation system was placed in the cell culture incubator at 37°C. After exposure to circulation for certain time, cells were collected and subjected to cell viability and apoptosis analyses.

Cell viability assay

Mouse CTCs and tumor cells were cultured as neurospheres in serum-free Neurobasal-A medium or as monolayers (for tumor cells only) in DMEM medium supplemented with 10% FBS. Cells were treated with TMZ (100 μmol/L; SelleckChem) for 48 hours, irradiated by 5-Gy X-ray with a dose rate of 2.8 Gy/min using an X-Rad 320ix cabinet system (Precision X-Ray), or placed in the *in vitro* circulation system. The cell viability was detected using a CellTiter-Glo Luminescent Cell Viability Assay Kit (Promega).

Cell apoptosis assay

Mouse CTCs and tumor cells were cultured in serum-free Neurobasal-A medium, and placed in the *in vitro* circulation system for 8 hours. Cells were stained with propidium iodide and FITC-conjugated Annexin V, followed by flow cytometry analysis with an Accuri C6 flow cytometer (BD Biosciences) by using FlowJo software.

Immunofluorescence

GBM was induced in *Ntv-a;Ink4a-Arf*$^{-/-}$;*Pten*$^{fl/fl}$;*LSL-luc* mice through RCAS/n-tva-mediated gene transfer. Tumors and blood CTCs were collected and transduced with adenovirus that encode TERT-Cherry. Cells were fixed with 4% paraformaldehyde for 15 minutes in room temperature, and treated with 0.25% Triton X-100 for 10 minutes for permeabilization, followed by incubation with anti-CD133 (1:100, Miltenyi, 130-092-442) and Alexa Fluor 488-conjugated anti-Olig2 antibody (1:100; Millipore, MABN50A4). Cells were stained with Alexa Fluor 568-conjugated secondary IgGs (1:500; Life Technologies) for 1 hour at room temperature, and mounted with the media containing DAPI. Images were acquired with an Axio Imager A1 upright fluorescence microscope (Zeiss) equipped with an Axiocam 506 cooled CCD camera (Zeiss).

Immunoblot analysis

Cultured mouse CTCs and tumor cells were lysed with a RIPA buffer containing protease inhibitor cocktail (Roche) on ice for 20 min. A total of 20 μg of protein was resolved by electrophoresis with precasted 4-15% SDS-PAGE gels (Bio-Rad), followed by transfer to PVDF membranes and protein blocking. The following antibodies were employed for immunoblot: anti-GAPDH (Cell Signaling Technology; 5174), anti-Oct4 (Cell Signaling Technology; 2840), and anti-Sox2 (Cell Signaling Technology; 2748S) antibodies at 1:1,000 dilution. Proteins were detected with HRP-conjugated antibodies specific for either rabbit or mouse IgG (Bio-Rad), followed by ECL development (GE Healthcare; RPN2232).

Immunohistochemistry

Paraffin tissue sections with mouse tumors were deparaffinized and rehydrated, and subjected to antigen retrieval in Target Retrieve Solution (DAKO; S1699) at 95°C for 20 minutes. For histology study, sections were stained with hematoxylin and eosin dyes. For IHC study, sections were blocked with 5% horse serum for 1 hour at room temperature, and incubated with anti-Ki67 (1:100; Millipore, AB9260) or anti-GFP (1:100; Millipore, 06-896) antibody overnight at 4°C, followed by staining with ImmPACT DAB (Vector Laboratories). Images were acquired with an AxioLab microscope (Zeiss) equipped with an AxioCam HRC CCD camera (Zeiss).

Sphere formation assay

CTCs and primary tumor cells were trypsinized and suspended in serum-free Neurobasal-A medium as single-cell suspensions, followed by seeding into six-well plates at 5,000 cells per well. The cells were treated with or without 1 μmol/L XAV939. After incubation for 8 days, the spheres were imaged and counted under an Axiovert 50 microscope (Zeiss) equipped with an AxioCam HRM CCD camera (Zeiss).

Limited dilution assay

In vitro limiting dilution assay was performed as previously described (18). Briefly, CTCs and primary tumor cells were trypsinized and suspended in serum-free Neurobasal-A medium as single-cell suspensions, followed by seeding into 96-well plates at 1, 5, 10, 20, 40, and 80 cells/well. The cells were treated with or without 10 μmol/L XAV939. After incubation for 10 days, the occurrence of spheres was observed under an Axiovert 50

microscope (Zeiss) and the wells with at least one sphere was recorded as positive.

LEF1 reporter assay

Renilla luciferase cDNA was subcloned into a pTopflash plasmid vector to replace original firefly luciferase. Mouse CTCs and tumor cells were cotransfected with the generated pLEF1-*Renilla* and a plasmid encoding β-gal by using Lipofectamine 2000 (Invitrogen). The activity of *Renilla* luciferase was detected 24-hour posttransfection with a Dual-Luciferase Reporter Assay System (Promega), and β-gal was used as an internal control.

Study approval

All experiments with mice were performed in accordance with a protocol approved by the Institutional Animal Care and Use Committee of the University of Pennsylvania and with the Guide for the Care and Use of Laboratory Animals (8th ed., The National Academies Press, 2011). The collection of human tissues in compliance with the tissue banking protocol was approved by the University of Pennsylvania Institutional Review Board, and written informed consent was obtained from each participant.

Statistical analysis

Comparison between groups were performed by Student *t* (unpaired two-tailed analysis) and log-rank (Mantel–Cox) tests using Prism software, and $P < 0.05$ was considered statistically significant.

Results

GBM CTCs are CSC-like cells

We initially investigated the potential egress of CSCs into circulation as CTCs in mouse gliomas. We took advantage of an orthotopic, genetically engineered murine GBM model with a native microenvironment, induced by the *RCAS/N-tva*-mediated somatic *pdgfb* gene transfer in *Ink4a-Arf*$^{-/-}$;*Pten*$^{-/-}$ neural stem/progenitor cells (11, 12). Before tumor transplantation into recipient mice, the tumor cells were transduced to express a genetic probe to trace cells with stemness activation (Fig. 1A), in

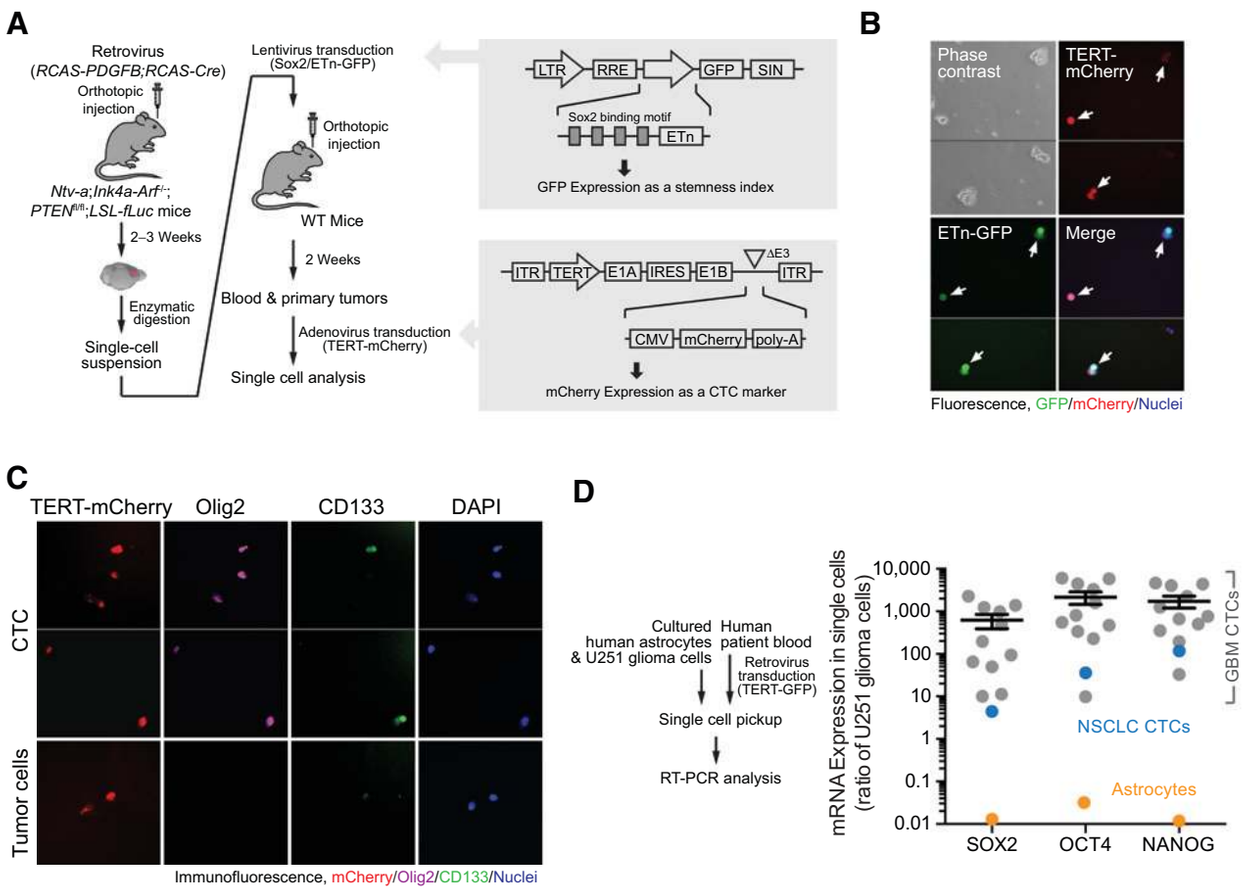

Figure 1.

Identification of glioma CTCs as CSC-like cells. **A–C,** The primary GBM in *Ntv-a;Ink4a-Arf*$^{-/-}$;*Pten*$^{fl/fl}$;*LSL-Luc* donor mice was induced by RCAS-mediated somatic gene transfer. Single-cell tumor suspension was transduced to express Sox2/Etn-GFP (**A** and **B**), or directly implanted into recipient mice (**C**). After tumor development in recipient mice, cells isolated from blood and tumors were transduced to express TERT-mCherry ($n = 4$ mice). **A,** Schematic approach. **B,** Blood cells were imaged. **C,** Blood and tumor cells were immunostained with anti-Olig2 and anti-CD133 antibodies. **D,** Blood samples from human patients with GBM or early stage NSCLC were transduced to express TERT-mCherry. mCherry^{+} cells were harvested by using a single-cell pickup system. As controls, single cells of human astrocytes and U251 glioma cells were also isolated. RNA was extracted, followed by RT-PCR analysis. mRNA expression was normalized with the GAPDH expression level and expressed as the ratios to U251 cells ($n = 11$ patients with GBM; mean ± SEM).

which GFP expression is driven by an early transposon promoter (Etn) with Sox2-binding motifs (19). CTCs harvested from the blood of the recipient mice were analyzed by a telomerase promoter-driven mCherry expression probe that is part of an adenoviral CTC-tagging system developed to detect human CTCs (7, 20). Notably, all mCherry$^+$ CTCs appeared to express GFP (Fig. 1B), whereas only 2% to 5% primary tumor cells express GFP (Supplementary Fig. S1), suggesting stemness transcriptional activation in glioma CTC cells. Moreover, immunofluorescence analysis showed that glioma CTCs, but not control primary tumor cells, robustly expressed stemness-associated transcriptional factor Olig2 (almost all cells; Fig. 1C) and a subpopulation of CTCs express glioma stem cell marker CD133 (about 40% cells), verifying that glioma CTCs are CSC-like. Furthermore, we investigated expression of stemness-associated transcriptional factors in human astrocytes or CTCs from patients with GBM or early stage NSCLC, related to the expression level of human U251 GBM cells, by using a single-cell microcapillary isolation system (Fig. 1D, left). Real-time RT-PCR analysis of pooled single cells revealed that GBM CTCs, and to a lesser extent, NSCLC CTCs, robustly expressed SOX2, OCT4, and NANOG, in contrast to a much lower expression of these genes in normal astrocytes (Fig. 1D, right), suggesting that human CTCs are also CSC-like.

We next established an optimized protocol to harvest and propagate CTCs *in vitro* (Fig. 2A). Cultured CTCs were able to form distinct neuropheres in serum-free stem cell medium *in vitro* (Fig. 2B). Interestingly, half of the spheres maintained long-term (4 weeks) Sox2/Etn-driven GFP expression after the probe transduction (Fig. 2B). Real-time RT-PCR analysis showed that these cultured CTCs consistently expressed Sox2, Oct4, and Nanog mRNA at high levels (Fig. 2C). The increased protein expression of Sox2 and Oct4 in CTCs were validated by immunoblot (Fig. 2D). In addition, we compared expression of these genes in mouse CTCs and human GBM CSCs. Our data show that GBM CTCs expressed SOX2 and OCT4 at a similar or higher level to CSCs, which was higher than the serum-treated, differentiated non-CSCs (Supplementary Fig. S2). Furthermore, as expected, treatment of these CTCs with 10% serum-supplemented medium altered their morphology from a neurosphere population to that of adherent and elongated cells (Supplementary Fig. S3); concomitantly, there was also an induced loss of Sox2/Etn-driven GFP expression, suggesting serum-induced differentiation in these cells.

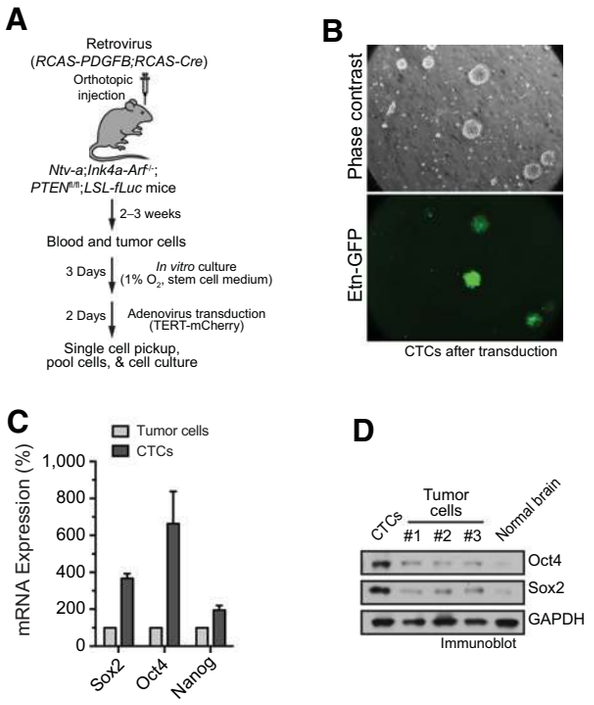

Figure 2.

In vitro cultured CTCs are CSC-like cells. GBM was induced in *Ntv-a*;*Ink4a-Arf*$^{-/-}$;*Pten*$^{fl/fl}$;*LSL-Luc* mice. After tumor development, cells isolated from blood and tumors were harvested, cultured, and transduced to express TERT-mCherry ($n = 5$ mice). **A,** Schematic approach. **B,** CTCs were transduced to express Sox2/Etn-GPF and cultured for 4 weeks, followed by imaging analysis. **C,** RNA was extracted from CTCs and matched tumor cells, and subjected to RT-PCR analysis. mRNA expression was normalized with the GAPDH expression level and expressed as the percentage of control ($n = 3$; mean ± SEM). **D,** CTCs and tumor cells were analyzed by immunoblot.

CTCs are highly tumorigenic and able to home to the primary tumor site

Next, we sought to investigate the tumorigenicity of CTCs by utilizing a subcutaneous implantation model (Fig. 3A) and an intracranial model (Supplementary Fig. S4A). Whole-body bioluminescence imaging of side-by-side subcutaneous tumors showed that implantation of CTCs developed significantly larger tumors than those derived from matched primary tumor cells (Fig. 3B). Moreover, the CTC-derived tumors grew faster than the tumor cell-derived tumors (Fig. 3C). Furthermore, mice with intracranial implantation of CTCs exhibited shorter survival than mice received tumor cell injection (Supplementary Fig. S4B), collectively suggesting a robust tumorigenic characteristic of these CTCs. Interestingly, CTC-derived tumors exhibited a highly invasive phenotype, as evidenced by invasion to adjacent muscle and blood vessel tissues (Fig. 3D). In addition, approximately 40% of the cells in CTC-derived tumors expressed proliferation marker Ki-67, indicating a highly proliferative nature, in comparison to a Ki-67 expression of about 20% of the cells in primary tumor cell-derived tumors (Supplementary Fig. S5).

Stem cells are known to be able to home to inflammatory, injured, or cancerous sites, when circulating in blood. Thus, we postulated that CSC-like glioma CTCs might be capable of seeding and colonizing a primary tumor, which could ultimately contribute to local GBM recurrence. To test this hypothesis, we generated genetically labeled CTCs that co-express GFP and *Renilla* luciferase (rLuc) under EF1 and CMV promoter, respectively, and via intravascular injection, administered these CTCs into a genetically engineered GBM mouse model in which tumor cells express firefly luciferase (fLuc; Fig. 4A). Whole-body bioluminescence imaging identified a distinct rLuc signal colocalizing with the fLuc-expressing primary tumor (Fig. 4B), indicating that CTCs had in fact homed to the intracranial tumor site. No other appreciable rLuc bioluminescence was observed in the body. Furthermore, IHC analysis of these tumors verified that these GFP$^+$ CTCs were localized in the border area of the primary tumor (Fig. 4C). Importantly, these experiments demonstrated that the CTCs colonized and formed a secondary tumor that invaded to the primary tumor. Together, these results suggest that CTCs are highly tumorigenic

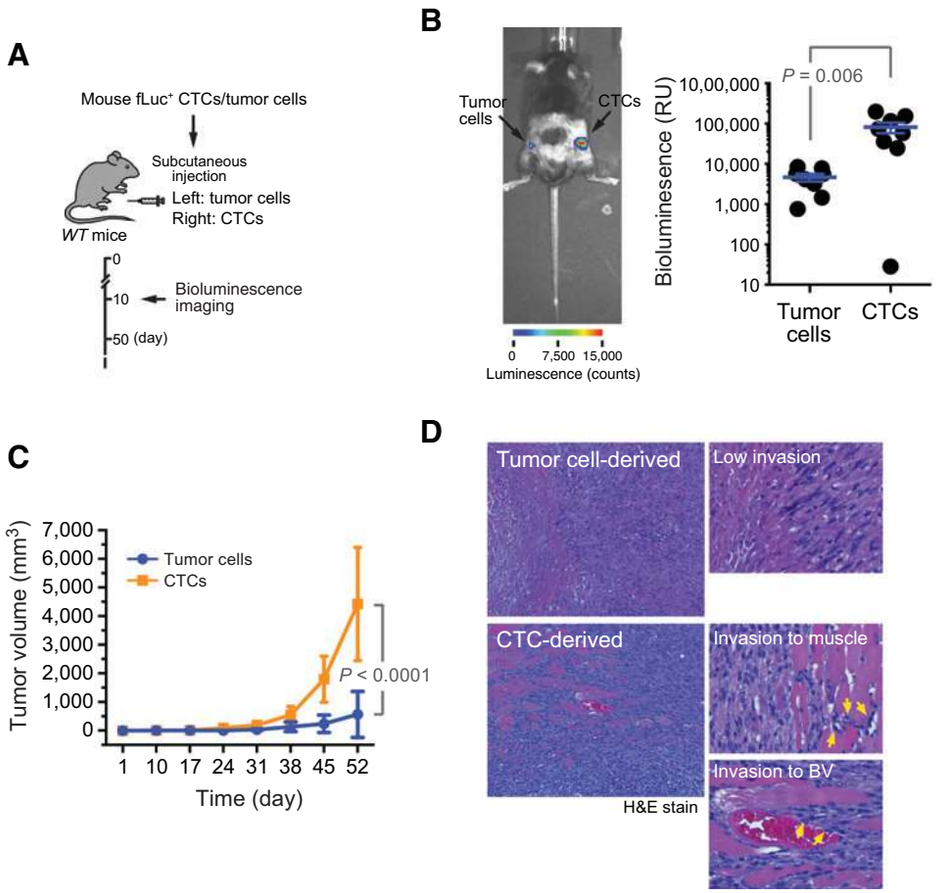

Figure 3.
CTCs are highly tumorigenic *in vivo*. **A–C**, Mouse CTCs and matched tumor cells were subcutaneously implanted into mice. **A,** Schematic approach. **B,** Mice were imaged by whole-body bioluminescence. Left, representative images. Right, quantified data ($n = 8$ mice from pooled two experiments, mean ± SEM). **C,** Tumor volume was measured over time ($n = 4$ mice; mean ± SEM). **D,** Tumor section was stained with hematoxylin and eosin (H&E) dyes. Arrows indicate the invasion.

and capable of homing to, and generating an additional tumor at the primary tumor site.

CTCs are resistant to cytotoxic treatments and circulation-induced stress

We next investigated the responses of CTCs to cytotoxic treatments. At the basal level without treatments, CTCs and control tumor cells exhibited a similar proliferative capacity when cultured in the same serum-free stem cell medium (Fig. 5A). Interestingly, CTCs were highly resistant to radiotherapy, as indicated by the doubling of viable CTCs 10 days after 5-Gy irradiation, compared to a more than 50% loss of viable tumor cells over the same period of time when cultured in the same serum-free stem cell medium or serum-containing DMEM medium (Fig. 5A). Similarly, CTCs were more resistant to treatment with temozolomide (TMZ), the agent for standard GBM chemotherapy, in comparison to tumor cells (Fig. 5B). These results suggest that CTCs are more refractory to cytotoxic treatments than

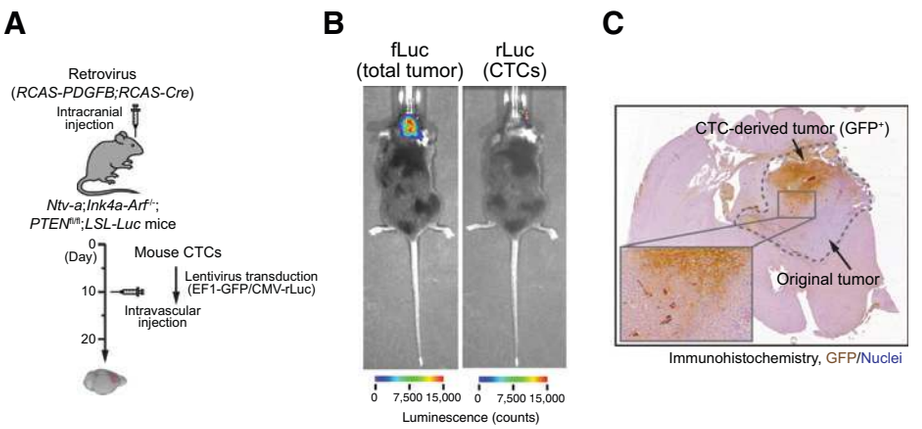

Figure 4.
CTCs are able to home to the primary tumor site. GBM was induced in *Ntv-a*; *Ink4a-Arf*$^{-/-}$;*Pten*$^{fl/fl}$;*LSL-Luc* mice. Mouse CTCs were lentivirally transduced to express CMV-GFP/rLuc, and intravascularlly injected into the mice with GBM tumors. **A,** Schematic approach. **B,** Mice were separately imaged by whole-body bioluminescence for fLuc and rLuc. Representative images are shown. **C,** Tumor section was immunostained with an anti-GFP antibody and counterstained with hemalin.

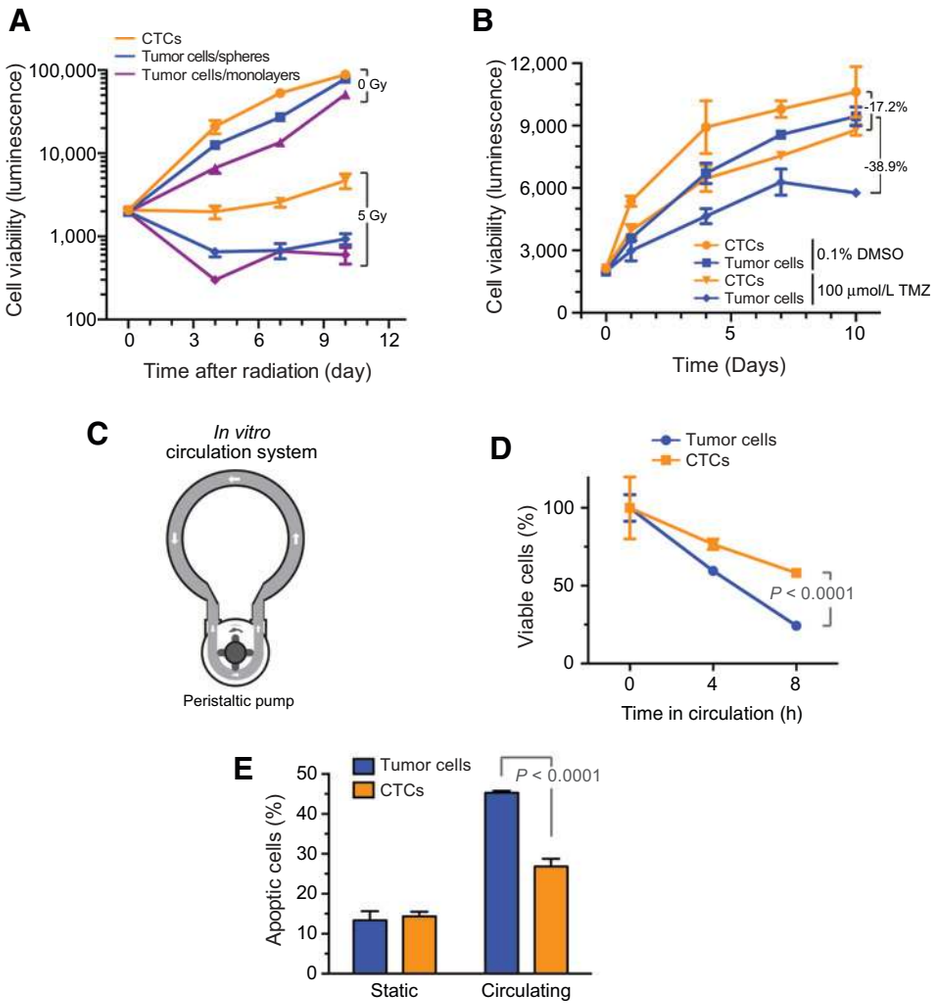

Figure 5.
CTCs are resistant to cytotoxic treatments and circulation-induced stress. **A,** Mouse CTCs and matched tumor cells that were cultured in serum-free stem cell medium as spheres, or as an additional control; the tumor cells were cultured in serum-containing DMEM medium to form monolayers. Cells were irradiated with or without 5-Gy X-ray. Cell viability was measured ($n = 3$; mean ± SD). **B,** Mouse CTCs and matched tumor cells were cultured in stem cell medium and treated with 100 μM TMZ or 0.1% DMSO. Cell viability was measured ($n = 3$; mean ± SEM). **C–E**, Mouse CTCs and matched tumor cells were cultured in stem cell medium and exposed to *in vitro* circulation. **C,** Schematic approach. **D,** Cell viability was measured after different treatment time in circulation ($n = 3$; mean ± SD). **E,** Cell apoptosis was analyzed after 8 hours in circulation ($n = 3$; mean ± SD).

their tumor cell counterparts. In addition, we compared the effects of circulation-induced stress on the viability of CTCs and tumor cells. To that end, we customized and built an *in vitro* circulation system by using 3-D printing materials (Fig. 5C). This system was operated with a fluid circulation rate of 80 mL/min, to model the blood flow in the middle arteries within normal human anatomy. Cell viability analysis showed that CTCs were capable of improved survival when compared to tumor cells in circulating medium (Fig. 5D). Consistent with these findings, circulation induced less cell apoptosis in CTCs than in tumor cells (Fig. 5E), suggesting that CTCs have higher tolerance to circulation-induced stress than tumor cells.

Single-cell RNA-seq analysis reveals Wnt activation in CTCs, inducing stemness and chemoresistance

We finally sought to explore the mechanistic underpinnings by which CTCs acquire stemness and develop treatment resistance by utilizing a CTC RNA-seq transcriptome analysis approach. Single CTCs were labeled by using the TERT-mCherry system and harvested (Fig. 6A). We succeeded in labeling and harvesting five to eight CTCs from each mouse. These cells were then pooled, and the extracted RNA subjected to linear amplification and deep sequencing (Fig. 6A). RNA-seq transcriptome analysis showed a change in global gene expression (Fig. 6B) and revealed that over 25% of total mapped genes had an over 60% change in expression levels (Fig. 6C). Moreover, CTCs and matched tumor cells from the same mouse exhibited distinct global expression profiles (Fig. 6D). Strikingly, computational bioinformatics analysis of the top 1,000 upregulated genes' promoter sequences in CTCs identified consensus DNA motifs that are known to be recognized by several transcriptional factors, including SP1 and LEF1 (Fig. 6E). Notably, LEF1 is the master transcriptional factor that controls Wnt signaling activation, which has a well-established role of Wnt in stemness and tumor treatment resistance. TOP-flash assays confirmed greater constitutive LEF1 activation in CTCs, compared to the matched tumor cells (Fig. 6F).

Interestingly, treatment of CTCs, but not tumor cells, with XAV939, a selective pharmacological inhibitor of Wnt pathway, remarkedly inhibited sphere formation (Fig. 7A). Likewise, limited dilution analysis showed that XAV939 treatment abrogated the stem cell frequency in CTCs but not in tumor cells (Fig. 7B), confirming that Wnt is critical for stemness activation in CTCs. Furthermore, XAV939 treatment sensitized CTCs, but not tumor cells, to TMZ chemotherapy (Fig. 7C), suggesting a requisite role of Wnt for chemoresistance in CTCs. In addition, XAV939 also inhibited neurosphere formation in human GBM CSCs

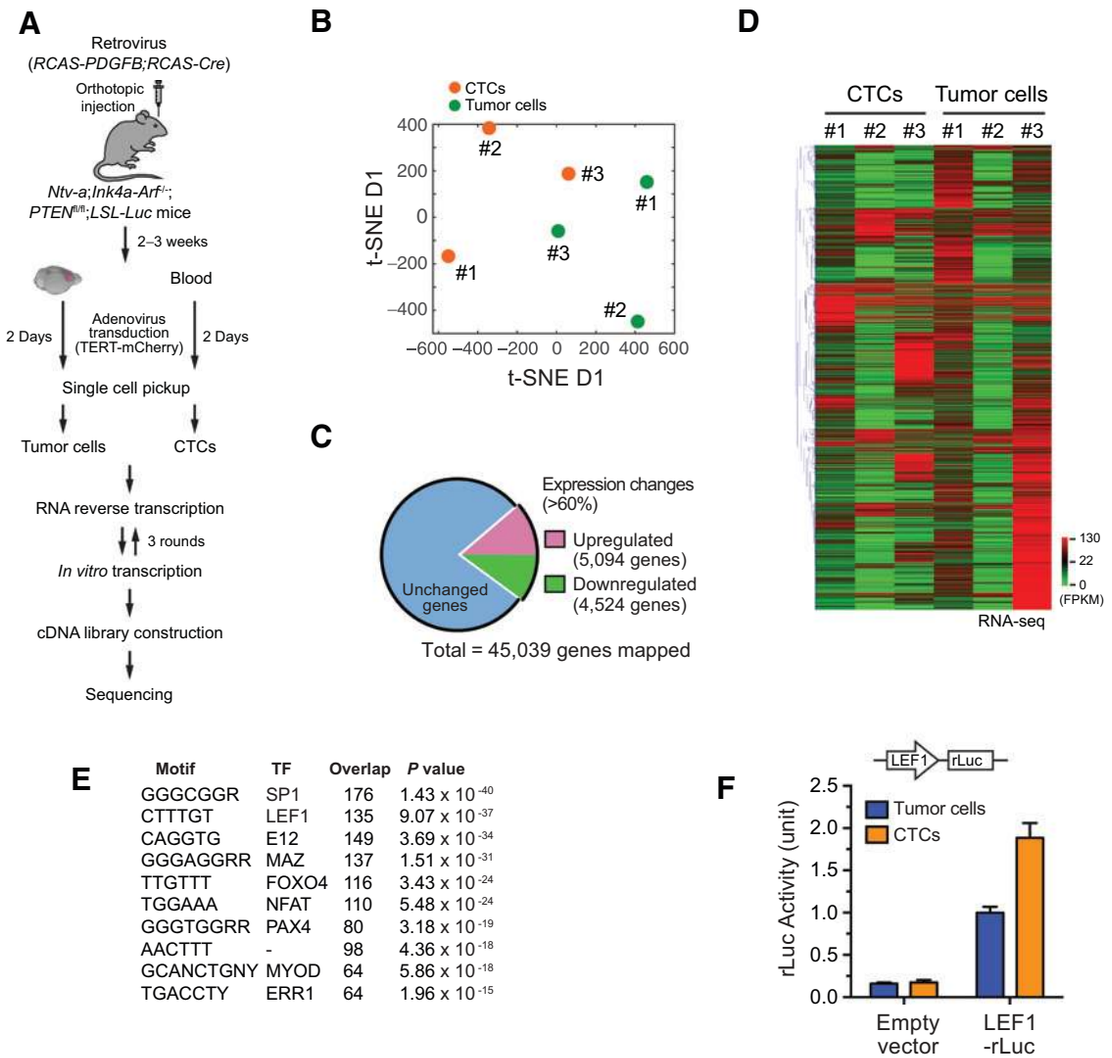

Figure 6.

Single-cell RNA-seq analysis reveals Wnt activation in CTCs. **A–E**, GBM was induced in Ntv-a;Ink4a-Arf-/-;Pten-/-;LSL-Luc mice. After tumor development, cells isolated from blood and tumors were transduced to express TERT-mCherry ($n = 3$ mice), followed by single-cell pickup. RNA was extracted from the isolated cells and subjected to three-round linear amplification. cDNA library was prepared and analyzed by deep sequencing. **A,** Schematic approach. **B–D**, Sequencing data was mapped and RNA expression quantified. **B,** t-SNE analysis of global expression exression. **C,** Global expression changes are shown. **D,** Expression of all genes was normalized with the GAPDH level of control tumor cells. The expression of changed genes (> 60%; CTCs versus matched tumor cells) is shown in a heat map. **E,** The promoter sequences of top 1,000 upregulated genes were analyzed through MSigDB database and most common motifs identified. The corresponding transcriptional factors are shown. **E,** Mouse CTCs and matched tumor cells were transduced with lentivirus encoding LEF1-rLuc or empty vector sequence. Luciferase activity was determined ($n = 3$; mean ± SD).

(Supplementary Fig. S6), suggesting a critical role for Wnt in stemness in both GBM CSCs and CTCs. Finally, we tested possible Wnt activation in GBM patient-derived CTCs. RT-PCR analysis demonstrated a robust expression of Wnt target genes including CCND1, CCND2, BTRC, and FGF9 in CTCs, compared with those in U251 glioma cells and human astrocytes (Fig. 7D), verifying Wnt activation in GBM patient-derived CTCs.

Discussion

CSCs play a critical role in treatment resistance and cancer recurrence. Here our study suggests that CSCs could egress from the tumor bulk into circulation as CTCs, survive in circulation during focal and systemic therapy, and re-seed the primary tumor bed to generate new local tumors, providing an alternative source for *in situ* tumor invasion. Maximal safe resection of the bulk tumor remains the standard of care in GBM and contributes to improved survival, but we speculate that CTCs may potentially return to the tumor bed via this reseeding mechanism, repopulate, and thus contribute to the universal recurrence rate seen in this disease.

Extracranial metastasis of GBM (EMG) is extremely rare, occurring in less than 2% of patients. This finding lends support to classical theories that patients have insufficient survival time for

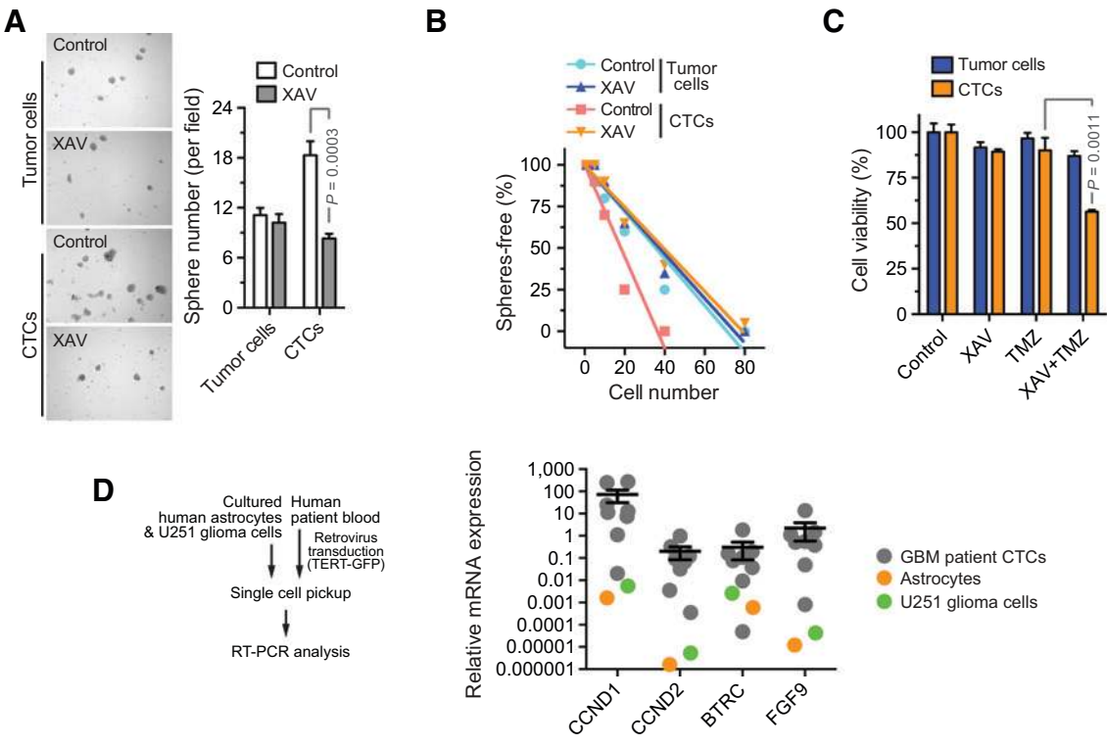

Figure 7.

Wnt activation induces stemness and chemoresistance in CTCs. **A** and **B**, Mouse CTCs and matched tumor cells were treated with 1 μmol/L XAV939 or control 0.1% DMSO. **A,** Cells were cultured for 8 days and imaged. Left, representative images. Right, quantified results ($n = 10$; mean ± SEM). **B,** Cells were subjected to limited dilution analysis. **C,** Mouse CTCs and matched tumor cells were treated with 10 μmol/L XAV939, 150 μmol/L TMZ, or both for 3 days. Cell viability was determined ($n = 3$; mean ± SD). **D,** Blood samples from human patients with GBM were transduced to express TERT-GFP. GFP^+ cells were harvested by using a single-cell pickup system. As a control, single-cell human astrocytes and U251 glioma cells were also isolated. RNA was extracted, followed by RT-PCR analysis. mRNA expression was normalized with the GAPDH expression level ($n = 8$ patients with GBM; mean ± SEM).

distant metastasis to manifest before they succumb to relapsed intracranial disease or that the presence of the blood–brain barrier (BBB) tends to limit hematogenous and lymphatic spread of CTCs (21, 22). Even so, the presence of glioma-derived CTCs has now been demonstrated by us and other independent groups (7, 23, 24). For example, a recent study showed that glioma CTCs occur much more frequently, as evidenced by detection of $GFAP^+$ CTCs in over 20% of patients with GBM (24). In accord, our previous work suggests that the sequential enumeration of telomerase transcription-tagged CTCs may correlate with treatment responses in patients with GBM (7). It is also noteworthy that patients with EMG or spinal metastasis show shorten survival time and poor response to radiotherapy (21, 25), collectively suggesting a potential pathologic role of CTCs in GBM tumor progression and recurrence. Although, we did not observe CTC seeding to other sites of the body in our mouse experiments, this may be influenced by the much shorter survival of mice compared to patients. We speculate that metastases to extracranial sites might have eventually occurred over a longer time period than what was tested in our model.

As a classic biological feature, stem cells can egress from bone marrow into circulation and home to injured or inflammatory sites (26, 27). Consistent with a recent study showing that *ex vivo* cultured colorectal CTCs express stem cell-associated markers (28), our studies characterize stemness in glioma CTCs, and more importantly, we reveal that glioma CTCs are able to home to the primary tumor site and contribute to tumor growth. Growing evidence suggests that CSCs are tumorigenic and refractory to conventional genotoxic treatments, significantly contributing to tumor recurrence after treatment (29–31). Thus, highly tumorigenic CTCs may play an unexpected role in GBM recurrence as a CSC reservoir, that is, forming a TMZ-resistant circulating subpopulation, evading local radiotherapy and ultimately re-seeding and colonizing the primary tumor site to form new tumors. Likewise, clinical and surgical pathology evidence suggests that extension of GBM throughout the brain is surprisingly pervasive, which might not be sufficiently explained by just direct high invasion of the tumor cells. It is tempting to speculate that a continual seeding of CTCs into the primary tumor bed may contribute to local micro-metastasis and CSC colony evolution-mediated GBM heterogeneity.

CSCs have been well characterized in GBM, whose stemness is subjected to regulation by developmental signaling including Wnt, Notch, and hedgehog (32–35). A recent study shows that noncanonical Wnt signaling in CTCs predicts antiandrogen resistance in prostate cancer cells (36). Here we identify that Wnt activation induces stemness and renders CTCs resistant to conventional treatment. Eradication of CTCs by targeting Wnt may therefore represent a paradigm-shifting therapeutic strategy for GBM, one of the deadliest human malignancies, and possibly

other solid tumors. We are in the process of investigating this therapeutic approach.

Disclosure of Potential Conflicts of Interest

M. Alonso-Basanta has received speakers bureau honoraria from Varian. D.M. O'Rourke reports receiving a commercial research grant from Novartis; has ownership interest (including stock, patents, etc.) in Isoma Diagnostics; is a consultant/advisory board member of Isoma Diagnostics; and has provided expert testimony for clinical expert testimony. G.D. Kao has ownership interest (including stock, patents, etc.) in Liquid Biotech USA. No potential conflicts of interest were disclosed by the other authors. J.F. Dorsey ownership interest (including stock, patents, etc.) in Liquid Biotech USA, Inc. No potential conflicts of interest were disclosed by the other authors.

Authors' Contributions

Conception and design: T. Liu, H. Xu, DM. O'Rourke, Y. Gong, G.D. Kao, J.F. Dorsey, Y. Fan

Development of methodology: T. Liu, M. Huang, W. Ma, D. Saxena, G.D. Kao, J.F. Dorsey

Acquisition of data (provided animals, acquired and managed patients, provided facilities, etc.): H. Xu, M. Huang, W. Ma, D. Saxena, R.A. Lustig, DM. O'Rourke, J.F. Dorsey

Analysis and interpretation of data (e.g., statistical analysis, biostatistics, computational analysis): T. Liu, H. Xu, Z. Zhang, DM. O'Rourke, L. Zhang, G.D. Kao, J.F. Dorsey

Writing, review, and/or revision of the manuscript: T. Liu, M. Alonso-Basanta, Z. Zhang, DM. O'Rourke, Y. Gong, G.D. Kao, J.F. Dorsey, Y. Fan

Administrative, technical, or material support (i.e., reporting or organizing data, constructing databases): T. Liu, J.F. Dorsey

Study supervision: T. Liu, G.D. Kao, J.F. Dorsey, Y. Fan

Acknowledgments

We are grateful to Eric Holland for providing RCAS-PDGF GBM model, to James Eberwine for single cell transcriptome analysis, and to Celeste Simon for helpful discussions. We acknowledge the Radiation Oncology Clinical Research Coordinators at the University of Pennsylvania for their contribution. This work was supported in part by National Institutes of Health grants R01NS094533 and R01NS106108 (to Y. Fan), R01CA201071 (to G. Kao and J. Dorsey), K08NS076548 and R01CA181429 (to J. Dorsey), and R01CA190415 (to L. Zhang), AACR Judah Folkman award (to Y. Fan), and B*Cured Foundation Brain Cancer Investigator Award (to Y. Fan).

The costs of publication of this article were defrayed in part by the payment of page charges. This article must therefore be hereby marked *advertisement* in accordance with 18 U.S.C. Section 1734 solely to indicate this fact.

Received February 27, 2018; revised August 29, 2018; accepted October 5, 2018; published first October 15, 2018.

References

1. Plaks V, Koopman CD, Werb Z. Cancer circulating tumor cells. Science 2013;341:1186–8.
2. Massague J, Obenauf AC. Metastatic colonization by circulating tumour cells. Nature 2016;529:298–306.
3. Pantel K, Speicher MR. The biology of circulating tumor cells. Oncogene 2016;35:1216–24.
4. Hodgkinson CL, Morrow CJ, Li Y, Metcalf RL, Rothwell DG, Trapani F, et al. Tumorigenicity and genetic profiling of circulating tumor cells in small-cell lung cancer. Nat Med 2014;20:897–903.
5. Cristofanilli M, Budd GT, Ellis MJ, Stopeck A, Matera J, Miller MC, et al. Circulating tumor cells, disease progression, and survival in metastatic breast cancer. N Engl J Med 2004;351:781–91.
6. de Bono JS, Scher HI, Montgomery RB, Parker C, Miller MC, Tissing H, et al. Circulating tumor cells predict survival benefit from treatment in metastatic castration-resistant prostate cancer. Clin Cancer Res 2008;14:6302–9.
7. Macarthur KM, Kao GD, Chandrasekaran S, Alonso-Basanta M, Chapman C, Lustig RA, et al. Detection of brain tumor cells in the peripheral blood by a telomerase promoter-based assay. Cancer Res 2014;74:2152–9.
8. Yu M, Bardia A, Wittner BS, Stott SL, Smas ME, Ting DT, et al. Circulating breast tumor cells exhibit dynamic changes in epithelial and mesenchymal composition. Science 2013;339:580–4.
9. Stupp R, Mason WP, van den Bent MJ, Weller M, Fisher B, Taphoorn MJ, et al. Radiotherapy plus concomitant and adjuvant temozolomide for glioblastoma. N Engl J Med 2005;352:987–96.
10. Stupp R. Effect of tumor-treating fields plus maintenance temozolomide vs maintenance temozolomide alone on survival in patients with glioblastoma: a randomized clinical trial. JAMA 2017;318:2306–16.
11. Charles N, Ozawa T, Squatrito M, Bleau AM, Brennan CW, Hambardzumyan D, et al. Perivascular nitric oxide activates notch signaling and promotes stem-like character in PDGF-induced glioma cells. Cell Stem Cell 2010;6:141–52.
12. Huang M, Liu T, Ma P, Mitteer RA Jr., Zhang Z, Kim HJ, et al. c-Met-mediated endothelial plasticity drives aberrant vascularization and chemoresistance in glioblastoma. J Clin Invest 2016;126:1801–14.
13. Bao S, Wu Q, McLendon RE, Hao Y, Shi Q, Hjelmeland AB, et al. Glioma stem cells promote radioresistance by preferential activation of the DNA damage response. Nature 2006;444:756–60.
14. Yan K, Wu Q, Yan DH, Lee CH, Rahim N, Tritschler I, et al. Glioma cancer stem cells secrete Gremlin1 to promote their maintenance within the tumor hierarchy. Genes Dev 2014;28:1085–100.
15. Eyler CE, Wu Q, Yan K, MacSwords JM, Chandler-Militello D, Misuraca KL, et al. Glioma stem cell proliferation and tumor growth are promoted by nitric oxide synthase-2. Cell 2011;146:53–66.
16. Wang Y, Xu H, Liu T, Huang M, Butter PP, Li C, et al. Temporal DNA-PK activation drives genomic instability and therapy resistance in glioma stem cells. JCI Insight 2018;3.
17. Spaethling JM, Na YJ, Lee J, Ulyanova AV, Baltuch GH, Bell TJ, et al. Primary cell culture of live neurosurgically resected aged adult human brain cells and single cell transcriptomics. Cell reports 2017;18:791–803.
18. Schonberg DL, Miller TE, Wu Q, Flavahan WA, Das NK, Hale JS, et al. Preferential iron trafficking characterizes glioblastoma stem-like cells. Cancer Cell 2015;28:441–55.
19. Hotta A, Cheung AY, Farra N, Vijayaragavan K, Seguin CA, Draper JS, et al. Isolation of human iPS cells using EOS lentiviral vectors to select for pluripotency. Nat Methods 2009;6:370–6.
20. Kojima T, Hashimoto Y, Watanabe Y, Kagawa S, Uno F, Kuroda S, et al. A simple biological imaging system for detecting viable human circulating tumor cells. J Clin Invest 2009;119:3172–81.
21. Lun M, Lok E, Gautam S, Wu E, Wong ET. The natural history of extracranial metastasis from glioblastoma multiforme. J Neurooncol 2011;105:261–73.
22. Ray A, Manjila S, Hdeib AM, Radhakrishnan A, Nock CJ, Cohen ML, et al. Extracranial metastasis of gliobastoma: Three illustrative cases and current review of the molecular pathology and management strategies. Mol Clin Oncol 2015;3:479–86.
23. Sullivan JP, Nahed BV, Madden MW, Oliveira SM, Springer S, Bhere D, et al. Brain tumor cells in circulation are enriched for mesenchymal gene expression. Cancer Discov 2014;4:1299–309.
24. Muller C, Holtschmidt J, Auer M, Heitzer E, Lamszus K, Schulte A, et al. Hematogenous dissemination of glioblastoma multiforme. Science translational medicine 2014;6:247ra101.
25. Vertosick FT Jr., Selker RG. Brain stem and spinal metastases of supratentorial glioblastoma multiforme: a clinical series. Neurosurgery 1990;27:516–21; discussion 21–2.
26. Chute JP. Stem cell homing. Curr Opin Hematol 2006;13:399–406.
27. Christopherson KW 2nd, Hangoc G, Mantel CR, Broxmeyer HE. Modulation of hematopoietic stem cell homing and engraftment by CD26. Science 2004;305:1000–3.
28. Grillet F, Bayet E, Villeronce O, Zappia L, Lagerqvist EL, Lunke S, et al. Circulating tumour cells from patients with colorectal cancer have cancer stem cell hallmarks in ex vivo culture. Gut 2016.

29. Reya T, Morrison SJ, Clarke MF, Weissman IL. Stem cells, cancer, and cancer stem cells. Nature 2001;414:105–11.
30. Chen J, Li Y, Yu TS, McKay RM, Burns DK, Kernie SG, et al. A restricted cell population propagates glioblastoma growth after chemotherapy. Nature 2012;488:522–6.
31. Lathia JD, Mack SC, Mulkearns-Hubert EE, Valentim CL, Rich JN. Cancer stem cells in glioblastoma. Genes Dev 2015;29:1203–17.
32. Gong A, Huang S. FoxM1 and Wnt/beta-catenin signaling in glioma stem cells. Cancer Res 2012;72:5658–62.
33. Wang J, Wakeman TP, Lathia JD, Hjelmeland AB, Wang XF, White RR, et al. Notch promotes radioresistance of glioma stem cells. Stem Cells 2010;28:17–28.
34. Fan X, Khaki L, Zhu TS, Soules ME, Talsma CE, Gul N, et al. NOTCH pathway blockade depletes CD133positive glioblastoma cells and inhibits growth of tumor neurospheres and xenografts. Stem cells 2010;28:5–16.
35. Clement V, Sanchez P, de Tribolet N, Radovanovic I, Ruiz I, Altaba A. HEDGEHOG-GLI1 signaling regulates human glioma growth, cancer stem cell self-renewal, and tumorigenicity. Curr Biol 2007;17:165–72.
36. Miyamoto DT, Zheng Y, Wittner BS, Lee RJ, Zhu H, Broderick KT, et al. RNA-Seq of single prostate CTCs implicates noncanonical Wnt signaling in antiandrogen resistance. Science 2015;349:1351–6.